RI-003

An Inter-color CFA Interpolation using Local Map

Yuji Itoh†

1. Introduction

Single sensor digital cameras of consumer use generally employ color filter array (CFA) to represent multiple color spectral components, such as red, green, and blue. At the location of each pixel only one color sample is taken, and the other colors must be interpolated from neighboring samples. This color plane interpolation is known as CFA interpolation. The most commonly used CFA pattern is Bayer pattern [1]. As seen in Fig.1, in a Bayer pattern, green samples are obtained on a quincunx lattice (checkerboard pattern), and red and blue samples are on rectangular lattices.

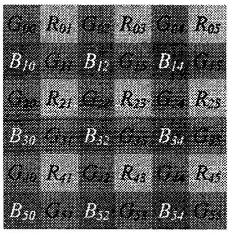

Fig. 1: Bayer CFA pattern with GRGR first row.

In the last two decades, various CFA interpolation methods have been proposed. Having reviewed recent literatures, we found that the most of the algorithms recently proposed belong to the edge-directed interpolation based on the inter-color correlation [2]-[4] and the bottom line is that the missing sample (or sample to be interpolated) must be interpolated from already available neighboring samples that are highly correlated with the missing pixel. We have found that finding the optimal direction of the interpolation filtering is the most critical problem for the CFA interpolation. The conventional inter-color methods apply the interpolation filtering either in horizontal-, vertical-, diagonal- or omni-direction (i.e. no preferred orientation) based on the decision of some orientation classifier. These methods are not optimal in the sense that the filtering cannot be applied in other direction than the pre-determined choices of the filtering directions.

In this paper, we propose a practical inter-color CFA interpolation scheme that uses a local map called unified geometry map (UGM) [5]. The UGM is an inter-color local map that is obtained from CFA data with a relatively simple operation. The proposed algorithm utilizes the UGM to decide which pixels are more correlated with the missing pixel. Thus, we have realized an inter-color CFA interpolation technique with flexible filtering directions. The rest of the paper is organized as follows. Section 2 studies prior arts in this field. Section 3 describes the concept and embodiment of the proposed algorithm, which is evaluated in Section 4. Finally we make some concluding remarks in Section 5.

2. Conventional CFA Interpolation

As we saw in the previous section, most of the recent papers address the edge-directed interpolation based on the inter-color correlation. Fig. 2 illustrates an inter-color CFA interpolation that projects a G sample value from the neighboring pixels in both intra- and inter-color channels. The pixel notation is: missing pixel (black circle), intra-color input pixels (white circle), and inter-color input pixels (white rectangular).

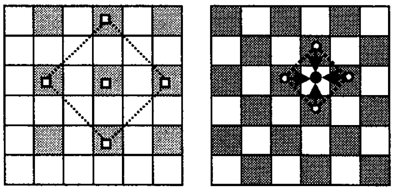

Fig. 2: Illustration of inter-color CFA interpolation.

The edge-directed inter-color methods apply the interpolation filtering either in horizontal, vertical, diagonal or entire directions (i.e., no preferred orientation) based on a decision by some orientation classifier. Typical orientation classifiers in horizontal direction, denoted by DH, at the R_{23} position in Fig. 1 are Eq. (1) for [2] and Eq. (2) for [3].

$$DH = |2 \cdot R_{23} - R_{21} - R_{25}| + |G_{22} - G_{24}| \tag{1}$$

$$DH = \begin{bmatrix} |2 \cdot R_{23} - R_{21} - R_{25}|/2 \\ + |G_{22} - G_{24}| + |2 \cdot G_{13} - G_{11} - G_{15}|/4 \\ + |2 \cdot G_{33} - G_{31} - G_{35}|/4 \\ + \left(|B_{12} - B_{14}| + |B_{32} - B_{34}| \right)/2 \end{bmatrix} /4 \tag{2}$$

The above orientation classifiers are intended to sense the high spatial frequency information present in the pixel neighborhood in the horizontal direction. The orientation classifiers in the other directions, such as one for the vertical direction denoted by DV, are calculated similarly in respective direction. Kuno *et al.* claim in [3] that their method is designed to function even in case of negative or no correlation (as well as positive correlation) whereas the conventional methods work only in case of high positive correlation. The filtering direction is, then, determined by using the orientation classifiers according to Eq. (3).

$$\begin{aligned} & \mathit{If}\ DH < DV \\ & \quad \mathit{horizontalfiltering} \\ & \mathit{else\ if}\ DV < DH \\ & \quad \mathit{verticalfiltering} \\ & \mathit{else} \\ & \quad \mathit{omni-directionalfiltering} \end{aligned} \tag{3}$$

Here we argue that these methods are not optimal in the sense that the filtering direction is chosen from among the pre-determined candidates even when the highest correlation exists in other direction that is not covered by the candidates.

Lukac *et al.* proposed so-called data adaptive filters (DAF) [4]. The uniqueness of the method mainly comes from an edge-sensing classifier called aggregated absolute differences, based on which the filtering masks and weighting coefficients are determined in a signal adaptive manner. This unique concept allows the filtering masks to be more flexible whereas most of the conventional methods select one among several pre-determined masks that are represented as filtering direction such

† Tsukuba University of Technology

as horizontal or vertical.

Here let us consider the population of the RGB vectors $x_{(i,j)} = [x_{(i,j)0}, x_{(i,j)1}, x_{(i,j)2}]$ with $x_{(i,j)k}$ indicating the R (k=0), G (k=1) and B (k=2) component at coordinates (i, j). The aggregated absolute differences at coordinates (i, j) in k-th color plane, which is denoted by $d_{(i,j)k}$, is obtained as follows.

$$d_{(i,j)k} = \sum_{(g,h)\in\varsigma} \left| x_{(i,j)k} - x_{(g,h)k} \right| \tag{4}$$

where ς represents the local vicinity, which is equivalent to the intra-color input pixels, around the missing pixel. Now let $\sigma_{(i,j)k}$ denote similarity measure at coordinates (i,j) in k-th color plane, which is generally expressed as a function of $d_{(i,j)k}$. Then, the weighting coefficients denoted by $w_{(i,j)k}$ of the adaptive interpolation filter is given by:

$$w_{(i,j)k} = \frac{1}{1 + d_{(i,j)k}} \tag{5}$$

The weighting coefficients need to be normalized. Finally, the DAF-CDM (DAF with color difference model) is performed by Eq. (6) (Note k=0 or 2).

$$\begin{aligned} x_{(s,t)k} &= x_{(s,t)1} + \sum_{(i,j)\in\varsigma} w_{(i,j)k} \cdot \left(x_{(i,j)k} - x_{(i,j)1} \right) \quad \text{for R and B} \\ x_{(s,t)1} &= x_{(s,t)k} + \sum_{(i,j)\in\varsigma} w_{(i,j)1} \cdot \left(x_{(i,j)1} - x_{(i,j)k} \right) \quad \text{for G} \end{aligned} \tag{6}$$

The DAF-CDM apparently belongs to the inter-color methods as shown by the above equations. However, the weighting coefficients are calculated in an intra-color fashion by Eqs. (4) and (5). Since the weighting coefficients are applied to signal difference between the color channels, we suppose that they should be obtained in an inter-color manner. In short, the DAF-CDM doesn't take full advantage of the inter-color correlation. The performance of the methods in [2], [3], [4] will be examined in the experiments later.

3. Proposed CFA Interpolation Algorithm

3.1 UGM-based CFA Interpolation

This section details how the proposed algorithm realizes a practical inter-color CFA interpolation using a local map called unified geometry map (UGM). An illustrative processing flow of the map index acquisition is depicted in Fig. 3. The map indices are obtained on M by N pixels block called UGM window (M=N=6 in Fig. 3). In each UGM window, a threshold value shall be determined first. In this study, we employ the average gray scale of pixels in the UGM window as threshold. Let τ_k be the average gray level of color k (R for k=0, G for k=1, B for k=2). Here, we calculate the map index at coordinates (i, j) denoted by $\lambda_{(i,j)}$:

$$\lambda_{(i,j)} = \begin{cases} 1 & if\ x_{(i,j)k} \geq \tau_k \\ 0 & otherwise \end{cases} \tag{7}$$

Fig. 4 shows the block diagram of the proposed algorithm set forth above. The algorithm is basically three-fold: i) map index acquisition, ii) global edge classification, and iii) UGM based interpolation. Here we assume that the input data are compatible with Bayer CFA pattern shown in Fig. 1. Note that we discuss the global edge classification after the map index acquisition and the UGM based interpolation for explanation ease.

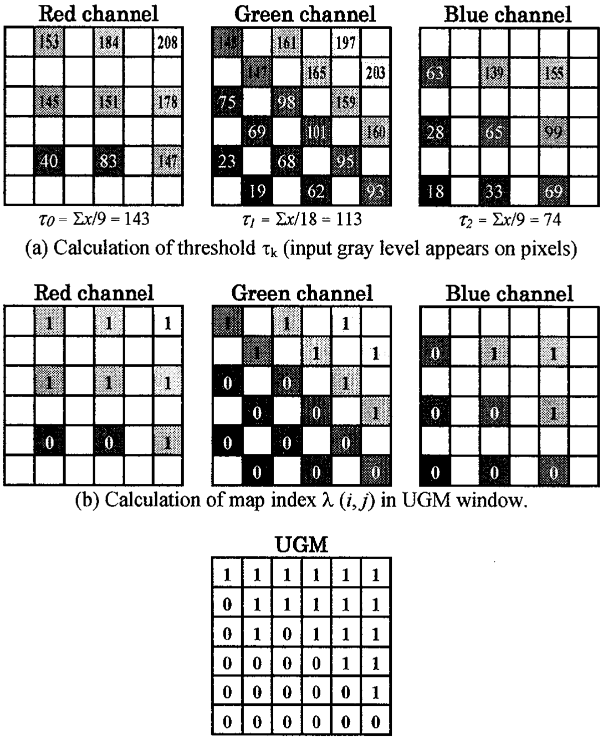

(a) Calculation of threshold τ_k (input gray level appears on pixels)

(b) Calculation of map index λ (i,j) in UGM window.

(c) Integration of three map index planes into UGM.

Fig. 3: Illustrative processing flow of map index acquisition.

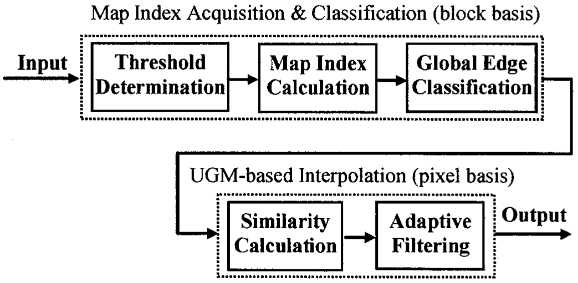
Map Index Acquisition & Classification (block basis)
Input
Threshold Determination
Map Index Calculation
Global Edge Classification
UGM-based Interpolation (pixel basis)
Similarity Calculation
Adaptive Filtering
Output

Fig. 4: Block diagram of proposed algorithm.

An example of a missing G pixel interpolation is explained using the CFA data and UGM depicted in Fig. 5. G_c is a missing pixel of the G channel collocated with A_c, where A is either R or B component. In the following equations, θ represents the similarity measure, and ζ denotes the local vicinity, which is equivalent to the input pixels, around the missing pixel (Fig. 6 depicts ζ in respective case).

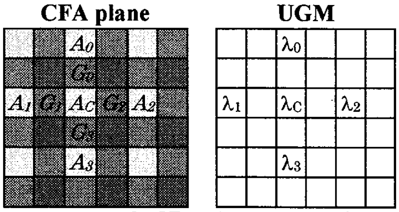

Fig. 5: Arrangement of CFA data and UGM to illustrate interpolation of a missing G pixel.

Now we calculate G_c according to Eq. (8), in which respective directional component and omni-directional component denoted by μ are added when θ=1 and θ=0, respectively.

$$G_c = \frac{1}{4}\sum_{l=0}^{3}\left\{\theta_l \cdot \left[G_l + (A_c - A_l)/2\right] + \bar{\theta}_l \cdot \mu\right\} \qquad (8)$$

$$\theta_l = \begin{cases} 1 & if\ \lambda_l = \lambda_c \\ 0 & otherwise \end{cases}$$

$$\mu = \frac{1}{4}\sum_{l=0}^{3}\left[G_l + (A_c - A_l)/2\right]$$

Similarly, the missing R (k=0) and B (k=2) pixels are obtained by:

$$x_{(s,t)k} = x_{(s,t)1} + \frac{1}{4}\sum_{(i,j)\in\varsigma}\left[\theta_{(i,j)} \cdot \left(x_{(i,j)k} - x_{(i,j)1}\right) + \bar{\theta}_{(i,j)} \cdot \rho\right] \qquad (9)$$

$$\theta_{(i,j)} = \begin{cases} 1 & if\ \lambda_{(i,j)} = \lambda_{(s,t)} \\ 0 & otherwise \end{cases}$$

$$\rho = \frac{1}{4}\sum_{(i,j)\in\varsigma}\left(x_{(i,j)k} - x_{(i,j)1}\right)$$

In this way, the proposed algorithm achieves as many as 15 (=2^4-1) filtering mask patterns whereas the conventional schemes examined earlier except the DAF-CDM have only 3 patterns, i.e., horizontal, vertical and omni-directional.

3.2 Global Edge Classification

The similarity measure denoted by θ in Eqs. (8) and (9) is calculated in a small region (5x5 at maximum). This makes the filtering sensitive to fluctuations in a small region, i.e. local structure, in some cases. Suppose that an edge runs vertically in the block concerned. In this case, the similarity measure suggests filtering vertically (i.e. along the edge) in most cases. However, it occasionally misleads to filtering horizontally (i.e. across the edge), which degrades the performance. Therefore, we introduce a measure based on a classifier called "global edge classifiers" that sense the structure of a broader region in order to avoid the above failure. The global edge classifiers, denoted by DH_{ge} and DV_{ge}, are calculated on the UGM window by:

$$DH_{ge} = \sum_{i=0}^{N-1}\sum_{j=0}^{M-2} f\left(\lambda_{(i,j)}, \lambda_{(i,j+1)}\right) \qquad (10)$$

$$DV_{ge} = \sum_{j=0}^{M-1}\sum_{i=0}^{N-2} f\left(\lambda_{(i,j)}, \lambda_{(i+1,j)}\right)$$

$$f(p,q) = \begin{cases} 1 & if\ p != q \\ 0 & otherwise \end{cases}$$

The similarity measure is, then, regulated by using the global edge classifiers according to Eq. (11). This process, i.e., enforcing particular similarity measures to be zero, is applied to Eq. (8) in calculating all the missing G pixels in the block concerned.

$$\begin{aligned} &If\ DH_{ge} + \delta < DV_{ge} \\ &\quad \theta_0 = \theta_3 = 0 \\ &else\ if\ DV_{ge} + \delta < DH_{ge} \\ &\quad \theta_1 = \theta_2 = 0 \end{aligned} \qquad (11)$$

3.3 Processing Details

Fig. 6 shows the UGM based interpolation process after the map index acquisition and the global edge classification are performed. Note that the acquisition of the map indices (A-stage), which corresponds to Fig. 3, is omitted in Fig. 6.

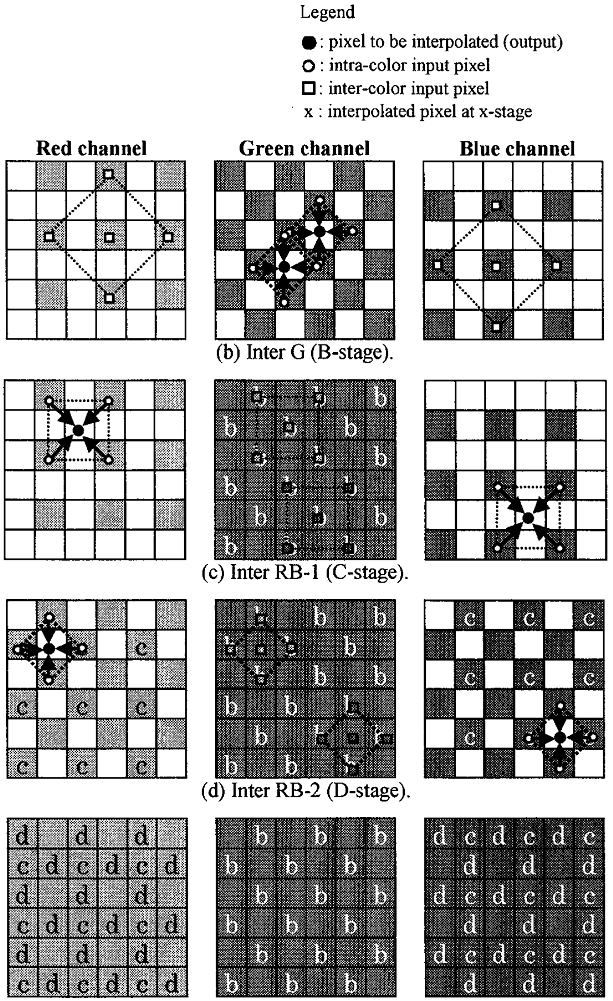
Legend
● : pixel to be interpolated (output)
○ : intra-color input pixel
□ : inter-color input pixel
x : interpolated pixel at x-stage
Red channel
Green channel
Blue channel
b
c
d

(b) Inter G (B-stage).

(c) Inter RB-1 (C-stage).

(d) Inter RB-2 (D-stage).

(e) Output.

Fig. 6: Processing flow of UGM based interpolation. The characters in a pixel represent the stage in which the pixel is interpolated, e.g. 'b' means that the pixel has been interpolated in B-stage.

1) Inter G (B-stage)

In Fig. 6 (b), let $\{G_c, G_0, G_1, G_2, G_3\} = \{x(s, t)_1, x(s\text{-}1, t)_1, x(s, t\text{-}1)_1, x(s, t+1)_1, x(s+1, t)_1\}$, and $\{Z_c, Z_0, Z_1, Z_2, Z_3\} = \{Z(s, t), Z(s\text{-}2, t), Z(s, t\text{-}2), Z(s, t+2), Z(s+2, t)\}$, where Z can be A sample, the map index λ, or the similarity measure θ. The missing G pixel at coordinates (s, t), denoted by G_c, is interpolated according to Eq. (8). Note that Eqs. (10) and (11) must be applied at the same time.

2) Inter RB-1 (C-stage)

Let ς = {(s-1, t-1), (s-1, t+1), (s+1, t-1), (s+1, t+1)} in Fig. 6 (c). The missing R pixel at coordinates (s, t) is interpolated according to Eq. (9). Similarly, interpolate the missing B pixels with k=2.

3) Inter RB-2 (D-stage)

Let ς = {(s-1, t), (s, t-1), (s, t+1), (s+1, t)} in Fig. 6 (d). The missing R pixel at coordinates (s, t) is interpolated according to Eq. (9). Similarly, interpolate the missing B pixels with k=2.

4. EXPERIMENTS

In the experiments, we measure the performance of the state-of-the-art CFA interpolations algorithms: bi-linear, the method in [2], the method in [3], DAF-CDM [4], and the proposed method with M=N=8 and δ=4 configuration, and compare them quantitatively. We use the *peak-signal to noise ratio* (PSNR) for the performance comparison, where the PSNR is given by (12).

$$PSNR = 10 \cdot \log_{10} \frac{255^2}{\frac{1}{3ST}\sum_{k=0}^{2}\sum_{s=0}^{S-1}\sum_{t=0}^{T-1}\left(o_{(s,t)k} - x_{(s,t)k}\right)^2} \tag{12}$$

where $\boldsymbol{o}_{(s,t)} = [o_{(s,t)0}, o_{(s,t)1}, o_{(s,t)2}]$ and $\boldsymbol{x}_{(s,t)} = [x_{(s,t)0}, x_{(s,t)1}, x_{(s,t)2}]$ denote the RGB vectors at coordinates (s,t) of the original image and processed image (both images are of extension S by T), respectively. We use 24 test images shown in Fig. 7, which are provided by Kodak. The input CFA data are captured from the original test images according to the Bayer CFA pattern shown in Fig. 1.

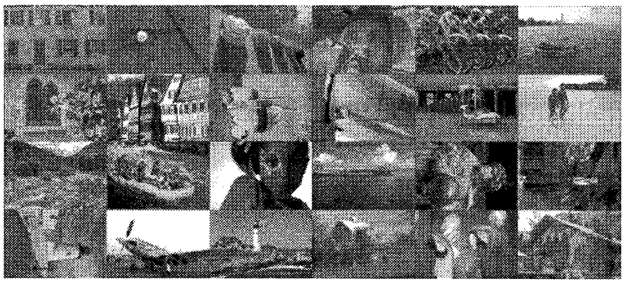

Fig. 7: Test images used for experiments. These are Kodak test images #1 through #24, from left to right, from top to bottom.

Table 1 summarizes the simulation results, in which the best scores per metric for each image is represented in bold. We observe several tendencies in the results: i) The method in [2] works well for the images with gentle or weak color transitions such as the test images #7 and #23, ii) The results of the method in [3] are synchronized with those of the method in [2], iii) The DAF-CDM doesn't work well for the images with steep or complicated color transitions such as the test images #8 and #13, iv) The proposed scheme yields the best score with over 87% probability (21/24 images) and tends to better handle complicated images, i.e., images with lower PSNRs, v) In PSNR wise, the proposed scheme outperforms the other methods by at least 1.0 dB on average. It can be concluded that the proposed method outperforms the other algorithms under test in terms of the PSNR.

Table 2 shows the normalized computations required to interpolate one missing pixel with regard to the primitive arithmetic operations. Then, we compare the proposed method with the state-of-the-art algorithms tested in the experiment above. This indicates that the proposed algorithm requires less computational resources than the DAF-CDM, and that the proposal is as inexpensive as the methods in [2] and [3]. It is noteworthy that the DAF-CDM necessitates multiplication and division that is one of the most resource hungry operations whereas the other schemes are free from multiplication and division.

Table 1: Simulation results, PSNR [dB].

Image Number	Bi-linear	Method in [2]	Method in [3]	DAF-CDM [4]	Proposed
1	26.37	33.91	34.13	34.52	**35.47**
2	33.46	39.67	39.73	**39.92**	39.87
3	34.65	40.68	40.55	40.84	**41.42**
4	33.95	39.60	39.53	39.72	**40.45**
5	26.82	35.09	35.39	35.11	**36.01**
6	28.02	35.07	35.46	35.62	**37.66**
7	33.61	41.01	**41.03**	40.23	40.99
8	23.82	32.48	32.61	32.35	**33.40**
9	32.67	40.23	40.12	40.70	**41.09**
10	32.63	40.14	40.23	40.53	**41.16**
11	29.40	36.43	36.66	36.59	**37.91**
12	33.55	40.89	40.69	41.14	**41.79**
13	24.05	29.96	30.05	29.76	**32.35**
14	29.52	35.82	35.86	35.77	**36.22**
15	32.46	37.94	37.86	38.09	**39.36**
16	31.49	38.67	39.07	39.31	**41.24**
17	32.28	38.64	38.69	39.30	**39.72**
18	28.19	33.99	34.09	33.65	**35.65**
19	28.33	37.42	37.54	37.71	**38.03**
20	31.81	38.55	38.72	38.96	**39.49**
21	28.71	35.48	35.60	36.02	**37.07**
22	30.68	36.61	36.66	36.89	**37.29**
23	35.23	**42.07**	41.93	41.72	41.96
24	26.64	31.69	31.60	31.30	**33.44**
Average	30.35	37.17	37.24	37.32	**38.29**
Note: The best score per image is represented in bold.					

Table 2: Normalized computations per pixel interpolation.

Operations Algorithm	shift	add / subtract	compare	absolute	multiply	divide
Method in [2]	3	10.3	0.93	2	0	0
Method in [3]	4.25	13.4	6.75	6.8	0	0
DAF-CDM [4]	0	29	0	6	4	8
Proposed	3.77	13.8	6.53	0	0	0

5. CONCLUSION

This paper has described a practical CFA interpolation technique that uses a local map called unified geometry map (UGM). We have confirmed through the simulations that the proposed algorithm outperformed the state-of-the-art technologies by 1.0 dB in terms of the PSNR. It has been also confirmed that the proposed algorithm is comparable to, or even less expensive than the state-of-the-art technologies with regard to the resource requirements. We will explore the CFA interpolation with multi-bit UGM in the further.

REFERENCES

[1] B.E. Bayer, "Color imaging array," U.S. Patent 3 971 065, July 1976.

[2] J.F. Hamilton Jr. and J.E. Adams, "Adaptive color plane interpolation in single sensor color electronic camera," U.S. Patent 5 629 734, May1997.

[3] T. Kuno and H. Sugiura, "Practical Color Filter Aarray Interpolation Part 2 with Non-linear Filter," IEEE Trans. Consumer Electron., vol.52, no.4, pp.1409-1417, Nov. 2006.

[4] R. Lukac and K.N. Plataniotis, "Data adaptive filters for demosaicking: A framework," IEEE Trans. Consumer Electron., vol.51, no.2, pp.560-570, May. 2005.

[5] Y. Itoh, "CFA Interpolation using Unified Geometry Map," Proc. FIT2008, RI-002, Sep. 2008.